Journal of Advanced Ceramics
2012, 1(2): 100-109
10.1007/s40145-012-0015-z ISSN 2226-4108

Review

Low-fired Y-type hexagonal ferrite for hyper frequency applications

Yang BAI[a,*], Wenjie ZHANG[a], Lijie QIAO[a], Ji ZHOU[b]

[a] *Key Laboratory of Environmental Fracture (Ministry of Education), University of Science and Technology Beijing, Beijing 100083, China*
[b] *State Key Lab of New Ceramics and Fine Processing, Department of Materials Science and Engineering, Tsinghua University, Beijing 100084, China*

Received June 3, 2012; Accepted July 12, 2012

Abstract: Y-type hexagonal ferrite with planar magnetocrystalline anisotropy has ultrahigh cut-off frequency up to GHz and excellent magnetic properties in hyper frequency range, so that is regarded as the most suitable material in correpongding inductive devices and components. The technology of low temperature cofired ceramics for surface-mounted multilayer chip components needs ferrite to be sintered well under 900 ℃ to avoid the melting and diffusion of Ag inner electrode during the cofiring process. To lower the sintering temperature of Y-type hexagonal ferrite, there are several methods, (1) using nano-sized starting powders, (2) substitution by low-melting elements, (3) adding sintering additives, and (4) introducing lattice defect. In this paper, the effects of different methods on the sintering behavior and the magnetic properties were discussed in detail.

Key words: hexagonal ferrite; magnetic material; low temperature cofiring ceramics

1 Introduction

With the development of modern electronic technology, the fast spread of portable electronic products promotes the trends of electronic technology towards miniaturization, integration and high frequency. The development of computer and wireless technology creates a great demand for novel chip inductive devices in hyper frequency, which need the magnetic material has excellent electromagnetic properties in hyper frequency. The mature spinel ferrites cannot serve as the suitable material in hyper frequency because the cubic magnetic structure limits their cut-off frequency below 100 MHz [1]. Soft-magnetic hexagonal ferrites, including Z-type and Y-type hexagonal ferrites, have a cut-off frequency one order of magnitude higher than that of spinel ferrites, so they are the desirable candidate for the inductive components in hyper frequency. Although Co_2Z, the most typical Z-type hexagonal ferrite, has high permeability in hyper frequency, its high sintering temperature beyond 1300 ℃ is hard to meet the need of low temperature cofired ceramics (LTCC) technology for surface-mounted multilayer chip components [2-5]. Hence, Y-type hexagonal ferrite becomes the best choice, because it has good magnetic properties in hyper frequency and relatively low

* Corresponding author.
E-mail: baiy@mater.ustb.edu.cn; Tel: 86-10-62334493;
Fax: 86-10-62332345

sintering temperature (~1150 ℃) [6-8].

The multilayer chip inductive components have complex structure with spiral inner electrode, which demands excellent cofiring match between electrode and magnetic material. For multilayer chip inductive components, such as multilayer chip inductor (MLCI) and multilayer chip beads (MLCB), Ag is the best choice as inner electrode, due to high electric and thermal conductivity. However, the melting and diffusion of Ag near the melting point can remarkably destroys the performance of devices [9,10], and its melting point of 961 ℃ is much lower than the sintering temperature of most ferrites. There are two solutions, raising the melting point of Ag or lowering the sintering temperature of ferrites. The melting point of silver alloy can be raised by noble metals, such as Pd, but the remarkable increment of price, about several dozens of times, prevents the application. Hence, it becomes the key in practical production of MLCI to lower the sintering temperature of ferrites to 900 ℃.

Sintering is an important process to create dense ceramics from powders [11]. The driving force for densification is the reduction of free energy by the decrease in surface area and the replacement of solid-vapor interfaces (particle surface) by solid-solid interfaces (grain boundary). The sintering process carries out based on mass transfer, either in liquid phase or solid phase, where the former is more efficient than the latter. Hence, both increasing the driving force and improving the mass transfer can promote the sintering process and lower the sintering temperature. The driving force of sintering can be raised effectively by adopting nano-sized starting powders with large surface area. The mass transfer in liquid phase can be promoted by substitution or sintering additives with low melting point. And the mass transfer in solid phase can be promoted by introducing specific defect in lattice, such as vacancy.

In this paper, some effective low firing methods are concluded, (1) nano technology, (2) substitution in lattice, (3) sintering additives and (4) lattice defect, where the effects on the sintering behavior and the magnetic properties were compared and discussed in detail.

2 Nano technology

The driving force of sintering can be great raised by using smaller starting particles with larger surface area, so using nano-sized particles, instead of micron-sized, can promote the sintering process and lower the sintering temperature. It also benefit the mass transfer in sintering process, which is affected by the change in pressure and differences in free energy across the curved surface [11]. These effects become larger in magnitude if the size of the particle is smaller, especially in nanoscale. Some researchers have reported the preparation of nano-sized Y-type hexagonal ferrite powders and corresponding electromagnetic properties [12-18]. Here, the powders prepared by citrate sol-gel process are set as example to clarify the effect of highly active nano-sized powders on phase formation, sintering behavior and magnetic properties.

Figure 1 shows the XRD pattern of the powders prepared by citrate sol-gel process and calcined at 900 ℃. As indexing by the standard XRD spectrum, the samples calcined at 900 ℃ are pure phase of Y-type hexagonal ferrite, where the temperature is about 100 ℃ lower than that of the micro-sized samples prepared by solid-state reaction method. The high activity of nano-sized powder promotes the mass transfer and solid state reaction, so the phase formation temperature is lowered obviously.

The large surface energy of nano-sized starting particles endows the sample high sintering activity, so they can be sintered well under low temperature. As shown in Fig. 2, the samples with nano-sized powders can be sintered well at 900 ℃, whose density is beyond 95% of theoretical density. In addition, the shrinkage rate is much larger than that of the sample

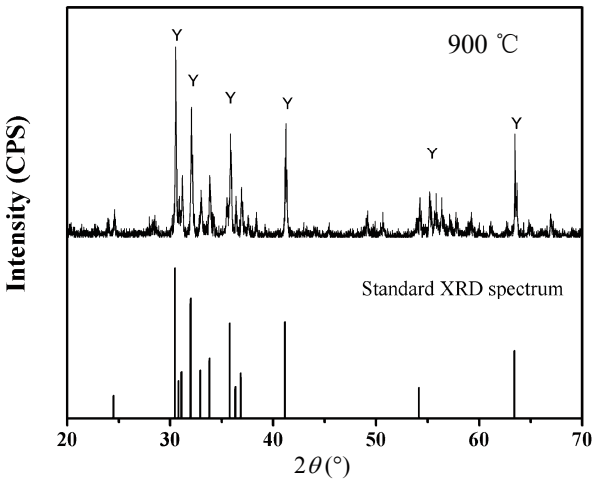

Fig. 1 XRD pattern of $Ba_2Zn_{0.8}Co_{0.8}Cu_{0.4}Fe_{12}O_{22}$ with nano-sized starting powders calcined at 900 ℃

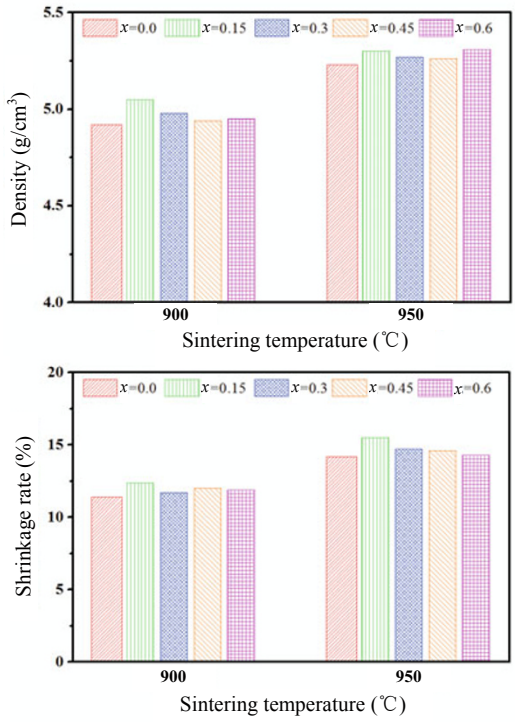

Fig. 2 Density and shrinkage rate of sol-gel method prepared $Ba_2Zn_{1.2-2x}Co_{2x}Cu_{0.8}Fe_{12}O_{22}$

using micron-sized powder sintered at high temperature.

Figure 3 compares the permeability of the samples made by different starting powders. To exclude the effect of microstructure on permeability, the samples with similar density are selected in the comparison, where the samples using nano-sized powders are sintered at 900 ℃, and those using micron-sized powders at 1000 ℃. The samples using nano-sized starting powders have higher permeability and the enhancement of permeability is notable for the samples with high Zn amount.

3 Substitution of low-melting elements in the lattice

The substitution of low-melting elements in ferrite can lower the sintering temperature effectively, because some liquid phase occurs at high temperature to promote the mass transfer in liquid phase during the sintering process. This method is convenient in the preparation process and facilitates to achieve homogeneous ion distribution and microstructure. However, its effect is often confined by the substitution limit associated with the difference of ion radii.

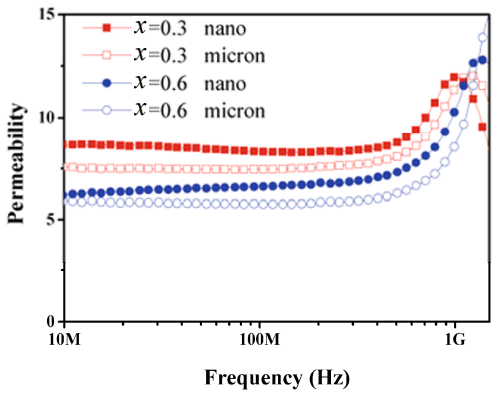

Fig. 3 Frequency dependence of the permeability of $Ba_2Zn_{1.2-2x}Co_{2x}Cu_{0.8}Fe_{12}O_{22}$ (x=0.3 and 0.6) prepared using different starting powders

3.1 Cu substitution

Cu^{2+} ion is the most common ion in ferrites and can lower the sintering temperature, because of the formation of liquid phase of Cu-containing compounds at high temperature. In addition, Cu ion has similar radius as Fe ion, which work for its substitution in ferrites. The Cu substation in spinel ferrites [19-23] and hexagonal ferrites [2-4,24,25], has been well studied, and it was proved efficient in Y-type hexagonal ferrites [6-8, 26-31].

Because the Cu-containing compounds with low melting temperature are formed to promote the mass transfer in liquid phase, the phase formation temperature is lowered effectively with Cu substitution. As shown in Fig. 4, $Ba_2Co_2Fe_{12}O_{22}$ without Cu substitution forms pure phase of Y-type hexagonal ferrite until 1050 ℃, while the temperature is lowered

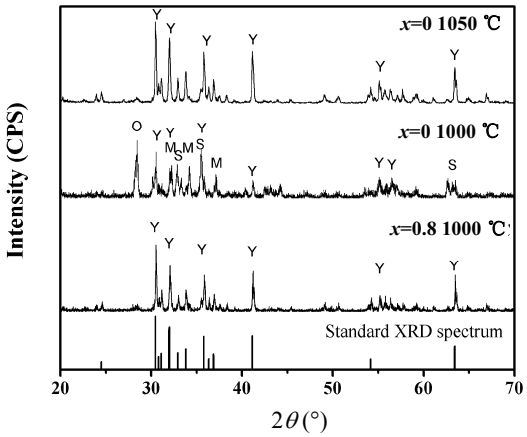

Fig. 4 XRD pattern of $Ba_2Co_{2-x}Cu_xFe_{12}O_{22}$ hexagonal ferrite calcined at different temperatures

to 1000 ℃ in $Ba_2Co_{1.2}Cu_{0.8}Fe_{12}O_{22}$ due to Cu substitution.

The dependences of shrinkage rate and density on the sintered samples, shown in Fig. 5, indicate the obvious effect of Cu substitution on lowering the sintering temperature. The higher the sintering temperature, the lower the sintering temperature is. The density of the sample with Cu amount of x=0.8 reaches 95% of theoretical density after sintered at 1000 ℃, which is 150 ℃ lower than that for the sample without Cu substitution. But Cu substitution is hard to lower the sintering temperature of Y-type hexagonal ferrite below 1000 ℃. The sintering temperature of pure Cu_2Y hexagonal ferrite ($Ba_2Co_{2-x}Cu_xFe_{12}O_{22}$) is just 1000 ℃.

The species and distribution of transition metal ions in ferrite determine the magnetic properties. In Y-type hexagonal ferrite, Co^{2+} and Zn^{2+} ions are the most efficient substitutions to modify magnetic properties. Co^{2+} ions help raising the planar anisotropy, which works for the rise of cut-off frequency and reduces the permeability. On the contrary, Zn^{2+} ions help increasing the saturation magnetization and reducing the magnetic anisotropy, so inverse effect is expected. Figure 6 shows the frequency dependence of the permeability of $Ba_2Zn_{1.2-x}Co_xCu_{0.8}Fe_{12}O_{22}$ hexagonal ferrites sintered at 1000 ℃. The permeability increases monotonically with the rise of Zn amount and the drop of Co amount.

Cu substitution in the Y-type hexagonal ferrite can also affect the magnetic properties. To avoid the effect of microstructure, the samples with similar density have been used in the comparison. Figure 7a indicates the effect of Cu substitution on Zn, which is shown that the permeability decreases with the rise of Cu substitution but the cut-off frequency raises, due to the reduction of saturation magnetization and the increase of anisotropy. Figure 7b shows the effect of Cu substitution on Co. The permeability increases slightly with the rise of Cu amount, because the reduction of Co amount declines the anisotropy. It is also found that the sample with high Zn amount is more sensitive to Cu substitution, because high Zn amount endows the samples low magnetic anisotropy.

3.2 Bi substitution

Bi_2O_3 is one of the most common sintering additives in ferrites and can efficiently lower the sintering temperature. Bi^{3+} can be also used as a substitution in the lattice of hexagonal ferrite. Pal and Winotaia reported the results with Bi substitution on Fe in M-type hexaferrite [32-35]. However, the valance variation of Bi and Fe ions destroys the dielectric character obviously, so such substitution is not suitable for the soft magnetic ferrite. In addition, Bi can also substitute for Ba due to their similar radius, which has been proved feasible in hexagonal ferrites, such as Y-type and Z-type hexagonal ferrites [36-38], to lower

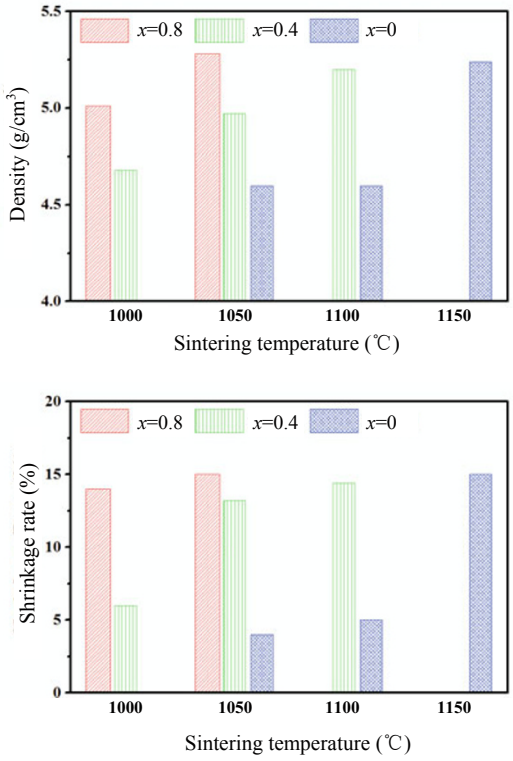

Fig. 5 (a) Densities and (b) shrinkage rate of $Ba_2Co_{0.6}Zn_{1.2-x}Cu_xFe_{12}O_{22}$ hexagonal ferrite sintered at different temperatures

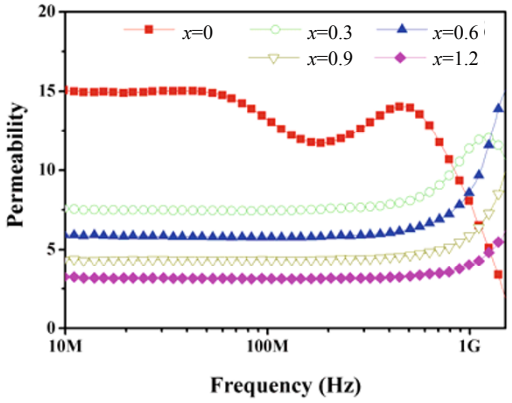

Fig. 6 Frequency dependence of the permeability of $Ba_2Zn_{1.2-x}Co_xCu_{0.8}Fe_{12}O_{22}$ sintered at 1000 ℃

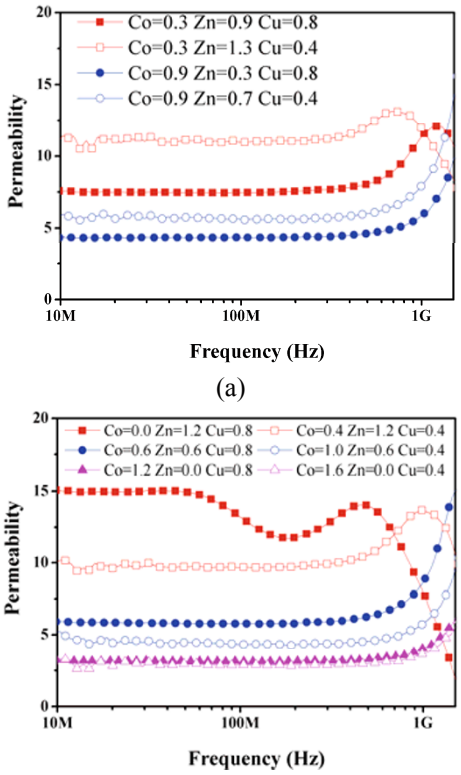

Fig. 7 Frequency dependence of the permeability of $Ba_2Zn_{2-x-y}Co_yCu_xFe_{12}O_{22}$. (a) Co amount is fixed; (b) Zn amount is fixed. The x=0.8 samples were sintered at 1000 ℃, and the x=0.4 samples at 1050 ℃.

the sintering temperature. Because the valences of Bi^{3+} and Ba^{2+} are different, identical amount of divalent ion with, such as Co^{2+} or Zn^{2+}, should substitute Fe^{3+} ion at the same time for the electrovalence balance.

Similar to Cu substitution, Bi substitution can also lower the phase formation temperature of Y-type hexagonal ferrite. As shown in Fig. 8, without the aid of Bi substitution, the pure phase of Y-type hexagonal ferrite does not be obtained after calcined at 900 ℃. However, minor Bi substitution can lower the phase formation temperature to 900 ℃ and shorten the calcination duration. And higher Bi amount benefits the phase formation more. As the Bi amount raise to x=0.15, the pure Y-type hexagonal ferrite is obtained after calcined at 900 ℃ for 0.5 h. However, excess Bi substitution may destroy the phase formation of Y-type hexagonal ferrite due to the difference of ion radius between Bi and Ba ions, and pure phase cannot be obtained as the amount of Bi is beyond x=0.3.

Figure 9 shows the densities and shrinkage rates of Bi substituted Y-type hexagonal ferrites. It is clear that Bi substitution can lower the sintering temperature

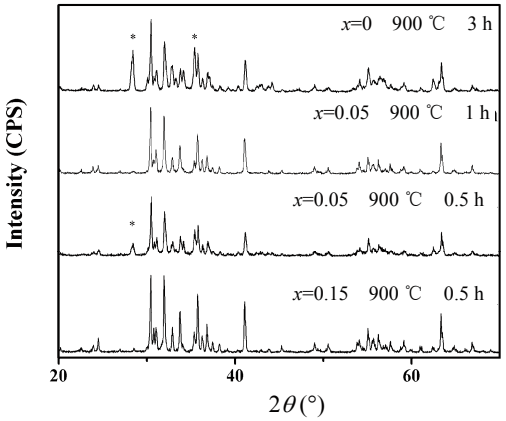

Fig. 8 XRD patterns of $Ba_{2-x}Bi_xZn_{0.8}Co_{0.8+x}Cu_{0.4}Fe_{12-x}O_{22}$ calcined at 900 ℃

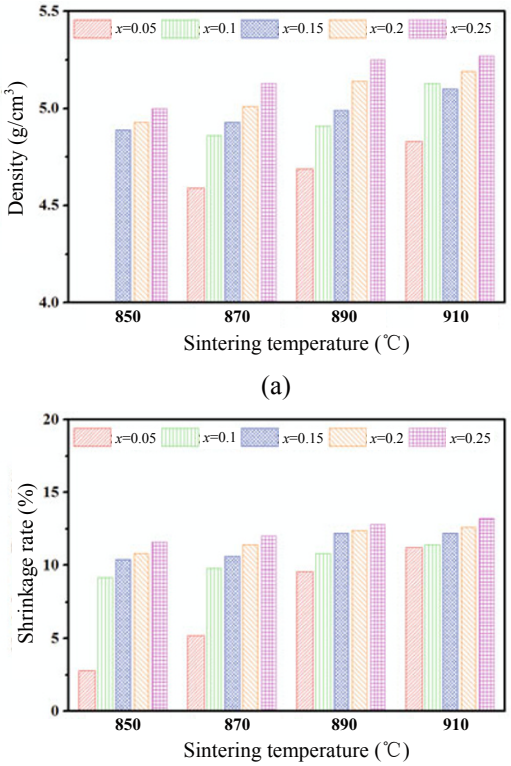

Fig. 9 (a) Densities and (b) shrinkage rates of $Ba_{2-x}Bi_xZn_{0.8}Co_{0.8+x}Cu_{0.4}Fe_{12-x}O_{22}$ hexagonal ferrite sintered at different temperatures

efficiently. The higher the Bi amount, the lower the sintering temperature is. The samples with minor Bi amount (x>0.05) can be sintered well under 900 ℃, which meets the need to cofire with Ag electrode in LTCC technology. The sintering temperature is lowered about 150 ℃ compared with that of the sample without Bi substitution.

Bi substitution also affects the magnetic properties

of Y-type hexagonal ferrites. Figure 10 shows the permeability of Y-type hexagonal ferrites with Bi-Co substitution and Bi-Zn substitution, where the samples with similar densification are selected in the comparison to exclude the influence of microstructure. The permeability declines monotonically with the rise of Bi-Co substitution, while it increases first, reaches a maximum at x=0.15, and then decreases for the Bi-Zn substitued samples. As the permeability may decrease with Co subtitution and increase with Zn substitution monotonically, the effect of Bi substitution on permeabiltiy is concluded to be negative. There may be two reasons, the internal stress due to the different ion radius and the change of magnetic ion distribution in the lattice. The relationship between permeability and internal stress can be expressed by

$$\mu \propto \frac{M_s^2}{K_1 + \lambda_s \sigma} \quad (1)$$

where M_s stands for saturation magnetization, K_1 for magneto-crystalline anisotropy, λ_s for magnetostriction factor and σ for internal stress. The substitution of Bi on Ba may induce internal stress in lattice due to ion radii difference, which makes permeability decline. On the other hand, the substitution in Ba site can change the ion distribution of transition metal ions in the interstitial site. For exsample, Sr substitution on Ba will make more Fe^{3+} into A sites antiparallel to the total magnetic moment, which make the permeability reduce.

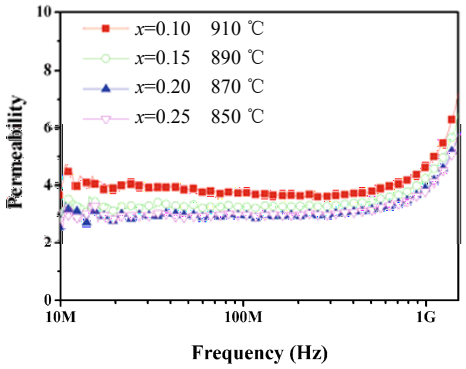

(a)

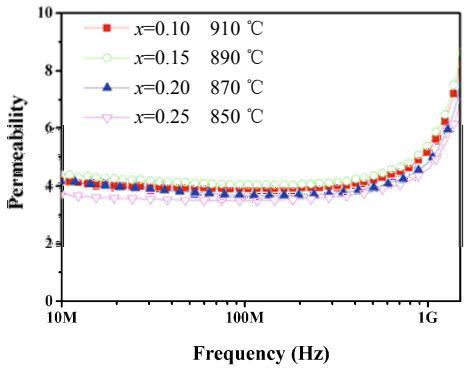

(b)

Fig. 10 Frequency dependence of the permeability of (a) $Ba_{2-x}Bi_xZn_{0.8}Co_{0.8+x}Cu_{0.4}Fe_{12-x}O_{22}$ and (b) $Ba_{2-x}Bi_xZn_{0.8+x}Co_{0.8}Cu_{0.4}Fe_{12-x}O_{22}$

4 Sintering additives with low melting point

Adding the low-melting sintering additives is the most common method to promote sintering process and lower the sintering temperature. After pure ferrite phase is formed after calcination, the additives are mixed with the ferrite powders during the second ball milling [39-43]. Different additives may play various roles in the sintering process. Some additive melts at high temperature, and promotes the mass transfer liquid phase. Some additive speeds up the solid state reaction by producing highly active interphase. Some additive accelerates the densification by large shrinkage when coating the ferrite particles. In general, the existence of liquid phase during sintering process is important for the sintering densification. Among various sintering additives, oxides and glasses with low melting point are most common. Here, Bi_2O_3 and B_2O_3-PbO glass are selected as examples.

Figure 11 compared the density and shrinkage rate of $Ba_2Zn_{1.2-x}Co_xCu_{0.8}Fe_{12}O_{22}$ with different sintering additives sintered at 870 ℃ for 6 h. The samples with same additives have similar density and shrinkage rate after sintered at same condition. As the sintering temperature is higher than 850 ℃, the samples with Bi_2O_3 doping have high densities beyond 5.0 g/cm^3 (about 93% of theory density), which proves the excellent low-firing effect of Bi_2O_3. Although the B_2O_3-PbO glass doped samples exhibits larger sintering shrinkage rate, but the density is not as high as expected. The shrinkage rate of the sample with 5wt% glass doping sintered at 870 ℃ for 6 h exceeds 13%, much larger than those of the Bi_2O_3 doped samples, but their densities are just under 4.85 g/cm^3 (about 88% of theory density).

The different sintering behavior originates from the different effects of sintering additives in sintering process. B_2O_3-PbO glass melts at lower temperature and coats the ferrite particles, which greatly promotes the sintering shrinkage but the densification of microstructure is far from sufficient. The effect of Bi_2O_3 is only to promote the liquid-phase mass transfer

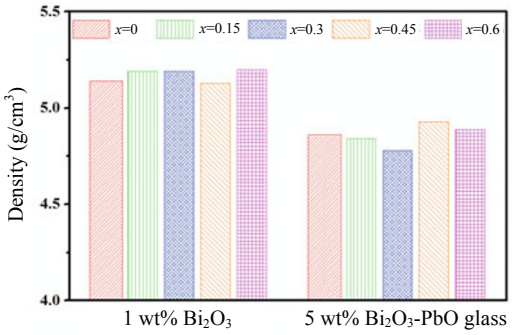

(a)

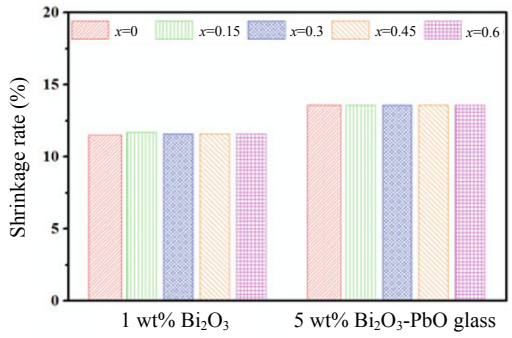

(b)

Fig. 11 (a) Densities and (b) shrinkage rate of $Ba_2Zn_{1.2-2x}Co_{2x}Cu_{0.8}Fe_{12}O_{22}$ with different sintering additives sintered at 870 ℃ for 6 h

at high temperature, and the amount is not enough to coat the ferrite particles.

The different effects of sintering additives also affect the magnetic properties. Figure 12 compares the permeability of the samples with different sintering additives. The permeability of the low-fired samples has similar frequency dispersion characters as those of the samples without additives and sintered at high temperature, but the value of permeability is lowered slightly. It is clear that the reduction of permeability is slight in the Bi_2O_3 doped samples, but severe in the glass doped samples. For example, the permeability of $Ba_2Zn_{1.2}Cu_{0.8}Fe_{12}O_{22}$ sintered at 1000 ℃ is 15, while that of 1wt% Bi_2O_3 doped samples sintered at 890 ℃ is 13, and that of 5wt% glass doped samples is only 5. That is beause that the mass of nonmagnetic glass coats the ferrit grain and blocks the magnetic current. On the other hand, the glass doped samples may have better dielectric and resistivity property, low due to the low permittivity and high resistivity of large amount of glass in the grain boundary.

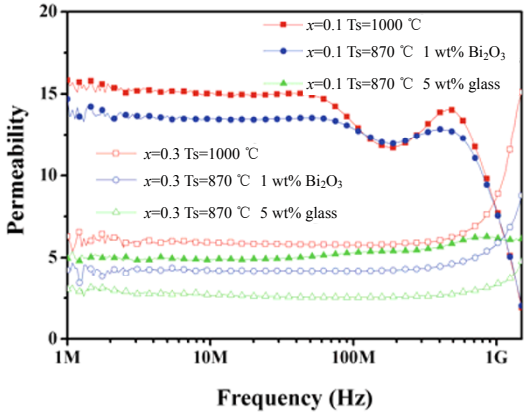

Fig. 12 Frequency dependence of the permeability of $Ba_2Zn_{1.2-2x}Co_{2x}Cu_{0.8}Fe_{12}O_{22}$ with different sintering additives

5 Lattice defect by nonstoichiometry

Mass transfer in solid phase is also an important process for sintering, which can be accelerated by ion vacancy. The ion vacancy includes cation vacancy and anion vacancy. Because anion vacancy can promote the valence variation of transition metal, which works against the electric properties, the cation vacancy is always used. The cation vacancy can be formed by the substitution of high-valence ions (W^{6+} etc.) and nonstoichiometric composition with cantion deficiency. Considering that the substitution of nonmagnetic ions may influence the magnetic properties, the Y-type hexagonal ferrites with Fe^{3+} cation deficiency ($Ba_2Zn_{0.6}Co_{0.6}Cu_{0.8}Fe_{12-x}O_{22-1.5x}$) were studied in some reports [44,45].

Fe^{3+} ions occupy the interstitial sites of the lattice, so small amount of cation deficiency does not damage the phase formation of Y-type hexagonal ferrite. Fig. 13 shows the XRD patterns of the samples with different cation deficiency. As $x \leqslant 1.0$, the phase

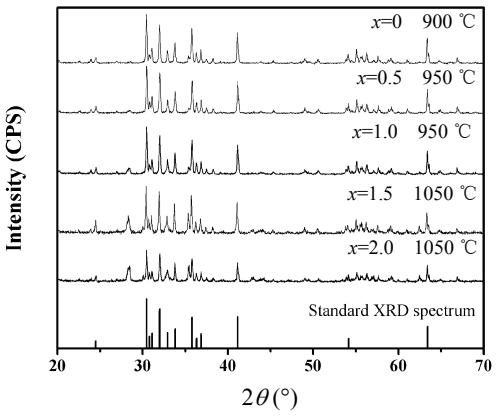

Fig. 13 XRD patterns of $Ba_2Zn_{0.6}Co_{0.6}Cu_{0.8}Fe_{12-x}O_{22-1.5x}$ calcined at 950℃ and 1050℃

formation is not affected and pure Y-type hexagonal ferrite can be formed at 1000 ℃ However, when the cation deficient ($x \geqslant 1.5$) is more, the phase formation will be destroy, and many other phases, such as $BaFe_2O_4$, always accompany with Y-type hexagonal ferrite although calcining temperature further rises to 1050 ℃.

Figure 14 shows the density and shrinkage rate of the samples sintered at different temperatures. It is clear that the samples with cation deficiency have much lower densification temperature because the mass transfer in solid phase is accelerated by ion vacancy during the sintering process. Their density and shrinkage rate are both much lower than those of the sample without cation deficiency. The samples with Fe^{3+} ion deficiency can be sintered well at 950 ℃, about 50 ℃ lower than the sample with stoichiometric proportion. It indicates that the ion vacancy can benefit the sintering process efficiently, but the effect on the mass transfer in solid phase is not quite as well as that in liquid phase, because the mass transfer in liquid phase is more crucial for the sintering process.

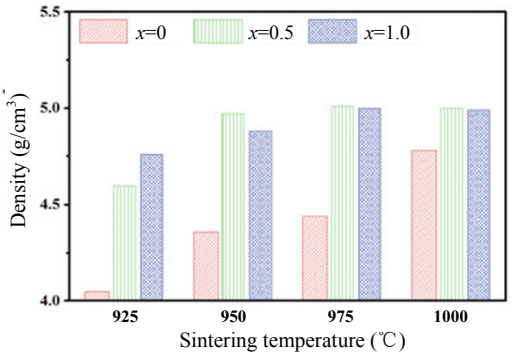

(a)

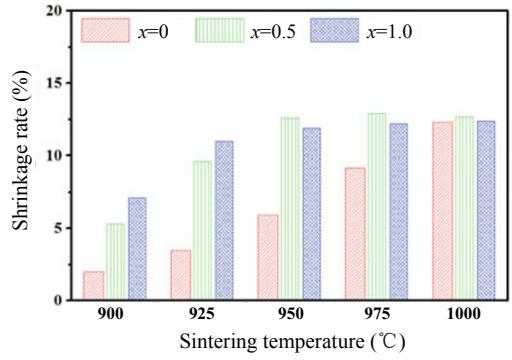

(b)

Fig. 14 (a) Densities and (b) shrinkage rate of $Ba_2Zn_{0.6}Co_{0.6}Cu_{0.8}Fe_{12-x}O_{22-1.5x}$ ($0 \leqslant x \leqslant 1.0$) sintered at different temperatures

Figure 15 shows the frequency dispersion of the permeability of the samples sintered at 950 ℃. All the samples exhibits stable permeability within 10 MHz to 1 GHz, and there is no obvious frequency dispersion. In addition, the magnetic low loss is low the in whole frequency range. All these will great benefit the application in hyper-frequency. Figure 16 compares the permeability (@300 MHz) of the samples sintered at different temperatures. The permeability of the x=0 samples with stoichiometric proportion increases linearly with the rise of sintering temperature due to the sintering densification. After sinter at 1000 ℃, the sample has a fully dense microstructure and the permeability reaches ~5.5. The permeability of the x=0.5 sample reaches a high value of ~5.8 at a low temperature of 950 ℃ because of its low densification temperature. For the x=1.0 samples, the permeability is always low, because the cation deficiency induces lattice stress to block the motion of domain wall and the spin rotation, and promotes the volatilization of Zn.

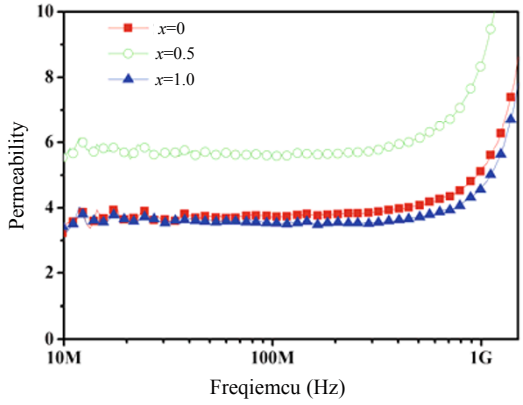

Fig. 15 Frequency dispersion of the permeability of $Ba_2Zn_{0.6}Co_{0.6}Cu_{0.8}Fe_{12-x}O_{22-1.5x}$ sintered at 950 ℃

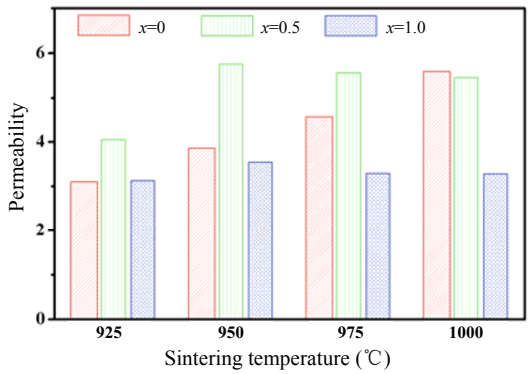

Fig. 16 Variation of permeability (@ 300MHz) of $Ba_2Zn_{0.6}Co_{0.6}Cu_{0.8}Fe_{12-x}O_{22-1.5x}$ sintered at different temperatures

6 Conclusions

Y-type hexagonal ferrite is a crucial magnetic material owing to its excellent magnetic properties in hyper frequency. It will play more and more important role in electronic industry with the trend towards high frequency. For its application in multilayer inductive devices, the low-firing technology is a key in LTCC. Lowering the temperature can be realized by either increasing the driving force of sintering or accelerating the mass transfer during the sintering process. Although there are several methods to lower the sintering temperature, the obtained low-fired samples have different electromagnetic properties. It is important to choose proper low-firing methods or their combination in practical application.

Acknowledgement

This work was supported by grants from the National Natural Science Foundation of China (No. 51172020), and the Fundamental Research Funds for the Central Universities (No. FRF-TP-09-028A).

Reference

[1] Smit J, Wijn HBJ. Ferrites. London, UK: Cleaver-Hume Press, 1959.

[2] Zhang HG, Zhou J, Wang YL, *et al*. Microstructure and physical characteristics of novel Z-type hexaferrite with Cu modification. *J Electroceram* 2002, **9**: 73-79.

[3] Zhang HG, Zhou J, Wang YL, *et al*. Investigation on physical characteristics of novel Z-type $Ba_3Co_{2(0.8-x)}Cu_{0.40}Zn_{2x}Fe_{24}O_{41}$ hexaferrite. *Mater Lett* 2002, **56:** 397-403.

[4] Zhang HG, Zhou J, Wang YL, *et al*. The effect of Zn ion substitution on electromagnetic properties of low-temperature fired Z-type hexaferrite. *Ceram Inter* 2002, **28:** 917-923.

[5] Kračunovska S, Töpfer J. Preparation, thermal stability and permeability behavior of substituted Z-type hexagonal ferrites for multilayer inductors. *J Electroceram* 2009, **22:** 227-232.

[6] Bai Y, Zhou J, Gui ZL, *et al*. An investigation of the magnetic properties of Co2Y hexaferrite. *Mater Lett* 2002, **57:** 807-811.

[7] Bai Y, Zhou J, Gui ZL, *et al*. Magnetic properties of Cu, Zn modified Co2Y hexaferrites. *J Magn Magn Materials* 2002, **246:** 140-144.

[8] Bai Y, Zhou J, Gui ZL, *et al*. Complex Y-type hexagonal ferrites: an ideal material for high frequency chip magnetic components. *J Magn MagnMater* 2003, **264:** 44-49.

[9] Lisjakw D, Drofenik M. Influence of Ag on the composition and electromagnetic properties of low-temperature cofired hexaferrites. *J Am Ceram Soc* 2007, **90:** 3121-3126.

[10] Lisjakw D, Drofenik M. Thermal stability of (Co,Cu)Z-Hexaferrite and its compatibility with Ag at 900°C. *J Am Ceram Soc* 2007, **90:** 3517-3521.

[11] Kingery WD, Bowen HK, Uhlmann DR. Introduction to Ceramics (2nd ed.). New York, US: John Wiley & Sons, Academic Press, 1976.

[12] Daigle A, DuPre E, Geiler A, *et al*. Preparation and characterization of pure-phase Co_2Y ferrite powders via a scalable aqueous coprecipitation method. *J Am Ceram Soc 2010*, **93:** 2994-2997.

[13] Zhang CX, Shi JS, Yang XJ, *et al*. Effects of calcination temperature and solution pH value on the structural and magnetic properties of $Ba_2Co_2Fe_{12}O_{22}$ ferrite via EDTA-complexing process. *Mater Chem Phys* 2010, **123:** 551-556.

[14] Nagae M, Atsumi T, Yoshio T. Preparation of Y-type barium hexaferrite by the glass-ceramic method. *J Am Ceram Soc* 2006, **89:** 1122-1124.

[15] Bai Y, Zhou J, Gui ZL, *et al*. Phase formation process, microstructure and magnetic properties of Y-type hexagonal ferrite prepared by citrate sol-gel auto- combustion method. *Mater Chem Phys* 2006, **98:** 66-70.

[16] Bai Y, Zhou J, Gui ZL, *et al*. Preparation and magnetic properties of Y-type ferroxplana by sol-gel method. *Key Eng Mater* 2005, **280-283:** 477-480.

[17] Cai JH, Dai LQ, Zhou XB. Thermodynamic analysis on preparation of zinc doped Co_2-Y planar hexagonal ferrite powder by chemical co-precipitation method. *Chinese J Inorg Chem* 2008, **24:** 1943-1948.

[18] Cai JH, Dai JQ, Chen WG, *et al*. Thermodynamic analysis on solubility of $Fe^{3+}/Ba^{2+}/Co^{2+}/Zn^{2+}/Cu^{2+}$ in NH_4HCO_3-NH_3 center dot H_2O and NaOH-Na_2CO_3 system. *Chinese J Inorg Chem* 2009, **25:** 886-892.

[19] Hsu JY. Low temperature fired NiCuZn ferrite. *IEEE T Magen* 1994, **30**: 4875-4877.

[20] Nam JH, Jung HH, Shin JY, *et al*. Effect of Cu substitution on the electrical and magnetic properties of NiZn ferrites. *IEEE T Magn* 1995, **31:** 3985-3987.

[21] Zhang HG, Ma ZW, Zhou J, *et al*. Preparation and investigation of $(Ni_{0.15}Cu_{0.25}Zn_{0.60})Fe_{1.96}O_4$ ferrite with very high initial permeability from self-propagated powders. *J Magn Magn Mater* 2000, **213:** 304-308.

[22] Low KO, Sale FR. The development and analysis of

property-composition diagrams on gel-derived stoichiometric NiCuZn ferrite. *J Magn Magn Mater* 2003, **256:** 221-226.

[23] Mürbe J, Töpfer J. High permeability Ni-Cu-Zn ferrites through additive-free low-temperature sintering of nanocrystalline powders. *J Euro Ceram Soc* 2012, **32:** 1091-1098.

[24] Wang XH, Ren TL, Li LT, *et al*. Synthesis of Cu-modified Co_2Z hexaferrite with planar structure by a citrate precursor method. *J Magn Magn Mater* 2001, **234:** 255-260.

[25] Kračunovska S, Töpfer J. Synthesis, sintering behavior and magnetic properties of Cu-substituted Co_2Z hexagonal ferrites. *J Mater Sci: Mater Electron* 2011, **22:** 467-473.

[26] Bai Y, Zhou J, Yue ZX, *et al*. Magnetic properties of composite Y-type hexagonal ferrites in a DC magnetic field. *J Appl Phys* 2005, **98:** 063901.

[27] Bai Y, Zhou J, Gui ZL, *et al*. The effect of Sr substitution on phase formation and magnetic properties of Y-type hexagonal ferrite. *J Am Ceram Soc* 2005, **88:** 318-323.

[28] Bai Y, Zhou J, Gui ZL, *et al*. Frequency dispersion of complex permeability of Y-type hexagonal ferrites. *Mater Lett* 2004, **58:** 1602-1606.

[29] Bai Y, Zhou J, Gui ZL, *et al*. Effect of substitution on magnetization mechanism for Y-type hexagonal ferrite. *Mat Sci Eng B* 2003, **103:** 115-117.

[30] Bai Y, Zhou J, Gui ZL, *et al*. Preparation and magnetic characterization of Y- type hexaferrites containing zinc, cobalt and copper. *Mat Sci Eng B* 2003, **99:** 266-269.

[31] Bai Y, Zhou J, Gui ZL, *et al*. Effect of Mn doping on physical properties of Y- type hexagonal ferrite. *J Alloy Comp* 2009, **473:** 505-508.

[32] Winotai P, Thongmee S, Tang IM. Cation distribution in bismuth-doped M-type barium hexaferrite. *Mater Res Bull* 2000, **35:** 1747-1753.

[33] Pal M, Brahma P, Chakravorty D, *et al*. Magnetic properties of Ba hexaferrites doped with bismuth oxide. *J Magn Magn Mater* 1995, **147:** 208-212.

[34] Pal M, Brahma P, Chakravorty D. Mixed valency character of bismuth in ferrite lattices. *J Mater Sci Lett* 1997, **16:** 270-272.

[35] Pal M, Brahma P, Chakraborty D, *et al*. DC conductivity in barium hexaferrites doped with bismuth oxide. *Jpn J Appl Phys* 1997, **36:** 2163-2166.

[36] Bai Y, Zhou J, Gui ZL, *et al*. The physic properties of Bi-Zn codoped Y-type hexagonal ferrite. *J Alloy Comp* 2008, **450:** 412-416.

[37] Bai Y, Zhou J, Gui ZL, *et al*. The effect of Bi substitution on phase formation and low temperature sintering of Y- type hexagonal ferrite. *J Electroceram* 2008, **21:** 349-352.

[38] Hsiang HI, Mei LT, His CH, *et al*. Crystalline phases and magnetic properties of Cu–Bi–Zn co-doped Co_2Z ferrites. *J Alloy Comp* 2011, **509:** 3343-3346.

[39] Pires GFM, Rodrigues HO, Almeida JS, *et al*. Study of the dielectric and magnetic properties of Co_2Y, Y-type hexaferrite ($Ba_2Co_2Fe_{12}O_{22}$) added with PbO and Bi_2O_3 in the RF frequency range. *J Alloy Comp* 2010, **493:** 326-334.

[40] Bai Y, Zhou J, Gui ZL, *et al*. Low-temperature sintered Y-type hexaferrites and their frequency properties. *J Func Mater* 2002, **33:** 487-489.

[41] Bai Y, Zhou J, Gui ZL, *et al*. Effect of Zn and Co doping on Co_2Y hexagferrite. *Piezoelectrics Acoustooptics* 2002, **24:** 135-138.

[42] Bai Y, Xu F, Ai F, *et al*. Study on physical Properties of low temperature sintered Co_2Y. *Piezoelectrics Acoustooptics* 2008, **30:** 335-336.

[43] Kračunovská S, Töpfer J. Co_2Z, Co_2Y and CoM-type hexagonal ferrites for multilayer inductors. *Key Eng Mater* 2010, **434-435:** 361-365.

[44] Bai Y, Zhou J, Gui ZL, *et al*. Electrical properties of non-stoichiometric Y-type hexagonal ferrite. *J Magn Magn Mater* 2004, **278:** 208-213.

[45] Bai Y, Zhou J, Gui ZL, *et al*. Magnetic properties of non-stoichiometric Y-type hexaferrite. *J Magn Magn Mater* 2002, **250:** 364-369.